JOURNAL OF MATERIALS SCIENCE 30 (1995) 776–783

The effect of trace additions of tellurium on oxidation and some other properties of aluminium–lithium base alloys

J. T. AL-HAIDARY, A. S. JABUR
Department of Production Engineering and Metallurgy, University of Technology, Baghdad, Iraq

Alloys of various chemical compositions with and without tellurium (Te) have been prepared in this research. Several types of tests were carried out, namely, tensile, ageing (hardness versus ageing time), erosion–corrosion, and oxidation, in addition to the evaluation of oxidation resistance by thermal shock. X-ray diffraction was also used to analyse the oxidation scales built on the samples. The microstructures of the alloys and oxides have been studied as well. It was found that the addition of small amounts (0.2 and 0.4 wt %) of Te led to drastic increases in oxidation resistance compared to the corresponding Te free alloy at both testing temperatures (300 and 500 °C). The great increase in resistance to environmental attack displayed by Te containing alloys was due to impediment of the interaction of Li with oxygen and enhancement of oxide plasticity and adhesion. Oxides grown on Te containing alloys remained intact when subjected to thermal shock. Te containing alloys also showed a great improvement in corrosion–erosion resistance compared to the other investigated Te free alloy. It was also noticed that Te enhanced the ductility of the base alloys themselves.

1. Introduction

One of the important application field of Al based alloys is the aerospace industry. Recently, a great attraction to these alloys has taken place due to principal improvements in their strength, toughness, thermal stability, as well as density. These improvements are achieved by production techniques and by the addition of lithium and other alloying elements. Aluminium alloys containing around 2 wt % lithium offer an attractive combination of mechanical properties, reduced density and increased elastic modulus [1–10]. However, some properties of Al–Li alloys may require substantial improvement. An important example of such a property is the high tendency of Al–Li alloys to oxidate [11–15], since Li additions exacerbate high temperature oxidation very much. This excessive reactivity can cause problems at all stages of processing and fabrication, particularly for thin alloy sections where the effects of Li depletion and intergranular oxidation are more severe; hence Li may diffuse to the surface and react with the atmosphere [14, 15].

Solution heat treatments are an integral part of the processing cycle of all age-hardening alloys, and all Al–Li alloys are age-hardenable. Rapid oxidation during the processing may lead to degradation of some properties [12–15]. As an example, oxidation increases with increasing percentage of Li in the alloy when the other conditions are the same [12, 14–17]. Previous work has shown that these alloys undergo rapid oxidation at solution heat treatment temperatures [13–15].

Some workers also reported that trace element additions of (Be, Ca, Bi) known to inhibit oxidation in certain aluminium alloys do not reduce oxidation in Al–Li alloys. Previous works [7, 16] have shown that substantial lithium loss may occur during solution treatment, and that this loss may result in a deterioration of mechanical properties near the surface [7, 12, 16]. The effect of germanium addition on the precipitation and deformation behaviours of Al–2% Li alloys has been studied by some workers [2, 3], and oxidation by others [11].

The present investigation is devoted to studying the influence of trace additions of Te on some properties of Al–Li based alloys, such as oxidation, erosion–corrosion, age-hardening, tensile and thermal shocks.

2. Experimental procedure

Alloys were prepared by casting in a steel mould under a controlled atmosphere in a specially designed apparatus. The chemical composition of the alloys is shown in Table I.

The alloys were homogenized at 550 °C for 18 h. Samples were then hot rolled up to 80% reduction. Samples of dimensions 100 × 20 × 2 mm were prepared. The solution heat treatment was for 1 h at 550 °C. The ageing temperature was 190 °C for all samples. Tensile specimens were chosen at peak

0022-2461

TABLE I Chemical composition of the alloys (wt %)[a]

Alloy code	Li	Cu	Mg	Zr	Te
V	0.0	4.0	0.0	0.2	0.0
W	2.0	1.0	2.0	0.2	0.0
X	2.0	1.0	2.0	0.2	0.2
Y	2.0	1.0	2.0	0.2	0.4

[a] Balance is Al.

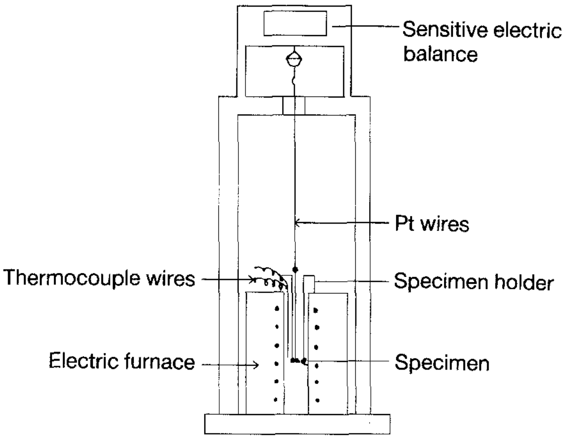

Figure 1 Block diagram of dry air oxidation system.

hardness conditions. Specimens were rectangular and prepared according to BS:18 Part 1, 1970. Three to four samples were tested in each case and the average values of elongation, tensile strength and yield strength were evaluated.

Microstructural studies were performed by optical microscopy (OM) and transmission electron microscopy (TEM) (Philips EM 301) at an operating voltage of 100 kV. Specimens for oxidation were cut from solution heat treated materials, then ground at finest silicon carbide paper (No. 1000). The oxidation test was carried out in dry air at 300 and 500 °C for 60 h. Specimens were put in the furnace after reaching the required temperature. A Pt–Pt/Rd thermocouple was put near the sample to measure the temperature accurately. The weight change was recorded to an accuracy of 0.1 mg (Fig. 1). The thermal shock test was conducted at two oxidation temperatures and after two periods of 50 and 60 h. The weight of each sample was initially recorded, then the sample was quickly removed from the furnace and allowed to cool to room temperature and then returned back to the furnace. Weight loss, if any, indicates the occurrence of spalling.

X-ray diffraction and scanning electron microscopy (SEM) were used to study the nature and topography of the oxides found on the specimens. The diffraction patterns were recorded using CuK_α radiation. The operating parameters were 40 kV, 20 mA.

In the erosion–corrosion test, samples were subjected to a jet of tap water at room temperature, Fig. 2. Weight losses were recorded after various exposure times. The weight loss per unit area and the weight loss per unit area per unit time were calculated.

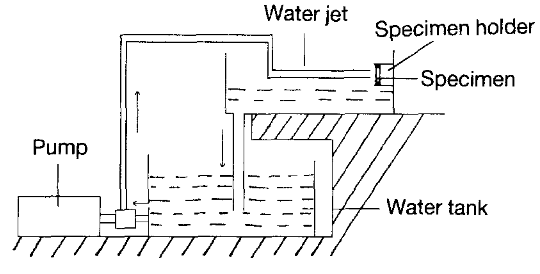

Figure 2 Block diagram of erosion–corrosion system.

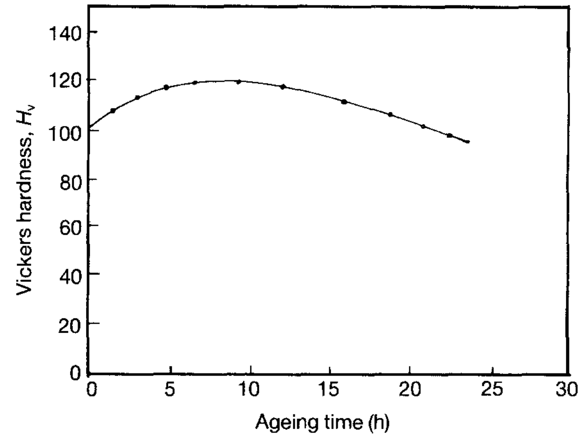

Figure 3 Hardness versus ageing time of alloy V.

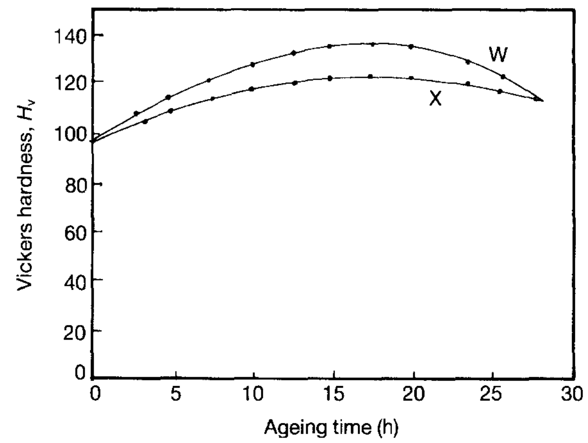

Figure 4 Hardness versus ageing time of alloys W and X.

3. Results and discussion

3.1. Thermal and mechanical behaviour

In the lithium free alloy (V), the variation of hardness with ageing time at 190 °C is shown in Fig. 3. It has been noticed that the substitution of 75% of Cu content by 2% Li and 2% Mg leads to an increase in the peak hardness and the time required to reach this point, Fig. 4. This means better thermal stabilities and mechanical properties, since the tensile strength of alloy W (lithium containing alloy) is higher than that of alloy V and the ductility of both alloys is the same (12%), as in Fig. 5 and 6.

There is no doubt that the density of alloy W decreased as the density of Li and Mg is 0.53 and 1.74 g cm^{-3} respectively. The decrease in density is an essential demand in aircraft alloys.

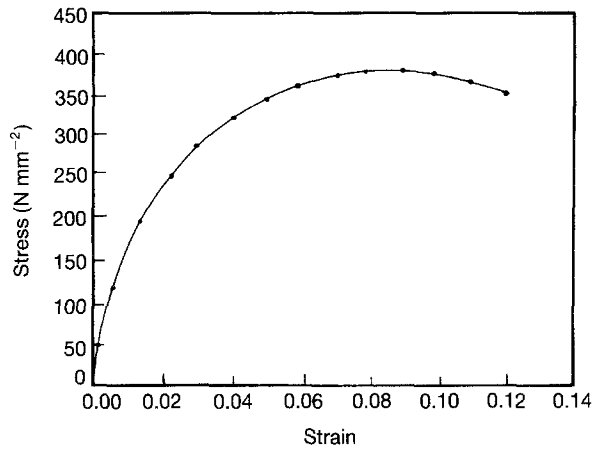

Figure 5 Stress–strain curve of alloy V.

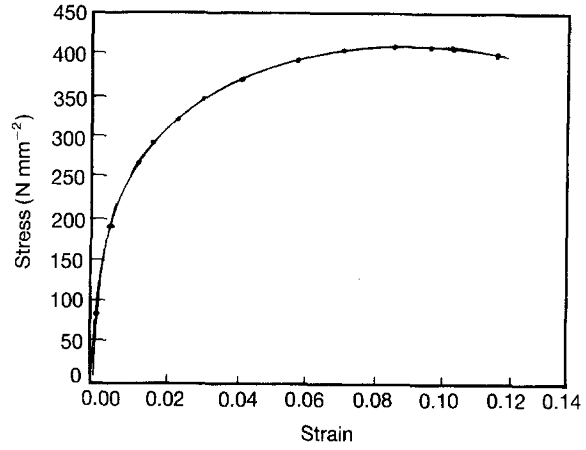

Figure 6 Stress–strain curve of alloy W.

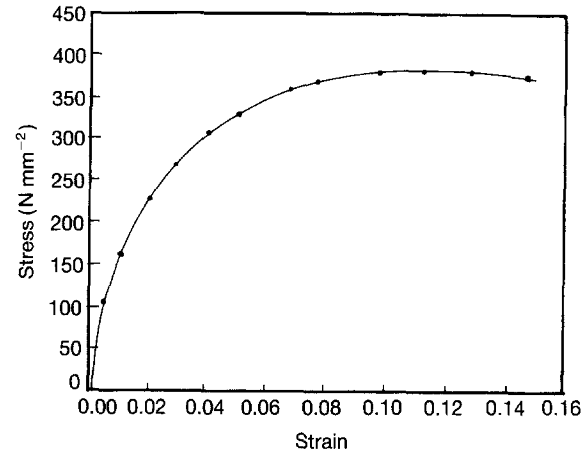

Figure 7 Stress–strain curve of alloy X.

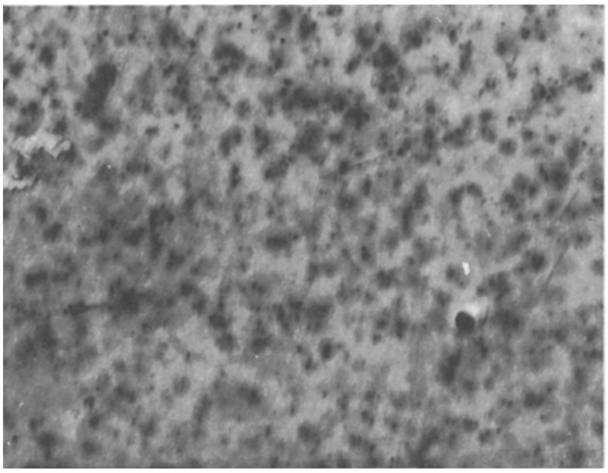

Figure 8 TEM image of a relatively large number of precipitates in Te free alloy at peak conditions (× 43 000).

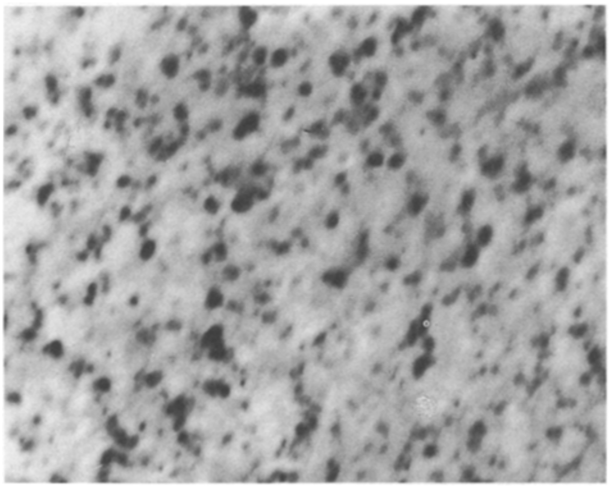

Figure 9 TEM image of a relatively low number of precipitates in Te containing alloy at peak conditions (× 43 000).

The addition of 0.2 wt % Te to allow W, producing alloy X, leads to a small decrease in the peak hardness value compared to alloy W. However, the rate of hardness decrease, after the peak, is lower in alloy X than in W, so that the two hardness values of both alloys are equal after 28 h. This indicates that the thermal stability of alloy X is even better than in W. Moreover, an improvement in ductility of the Te containing alloy (X) by 15% has been observed compared to that of alloy W (12%) under the same conditions (Figs 6 and 7). As a result, it has been found from the areas under the two curves (Figs 6 and 7), that the toughness of alloy X is higher than that of alloy W, which is another desirable property in aircraft industries. This may due to the effect of Te in the expansion of the lattice parameter of aluminium, and in turn decreases the stresses produced around the precipitates (stress relaxation during the precipitation process, as in the case of germanium addition [18]). This also leads to a relatively low amount of precipitation (Figs 8 and 9), and then lower hardness and strength to some extent. Due to this effect Te seems to encourage grain growth of the alloy (Fig. 10).

The other most probable mechanism of the Te role is that Te atoms may entrap Li atoms. As a result the concentration of Li atoms will be kept constant throughout surface layers, as well as in the interior of the sample, as indicated by microhardness measurements (Fig. 11).

Electron microscopy of specimens from the solution treated and overaged Te free alloy (W) revealed a narrow band relatively depleted of precipitates at the surface (Fig. 12), which also indicated the presence of

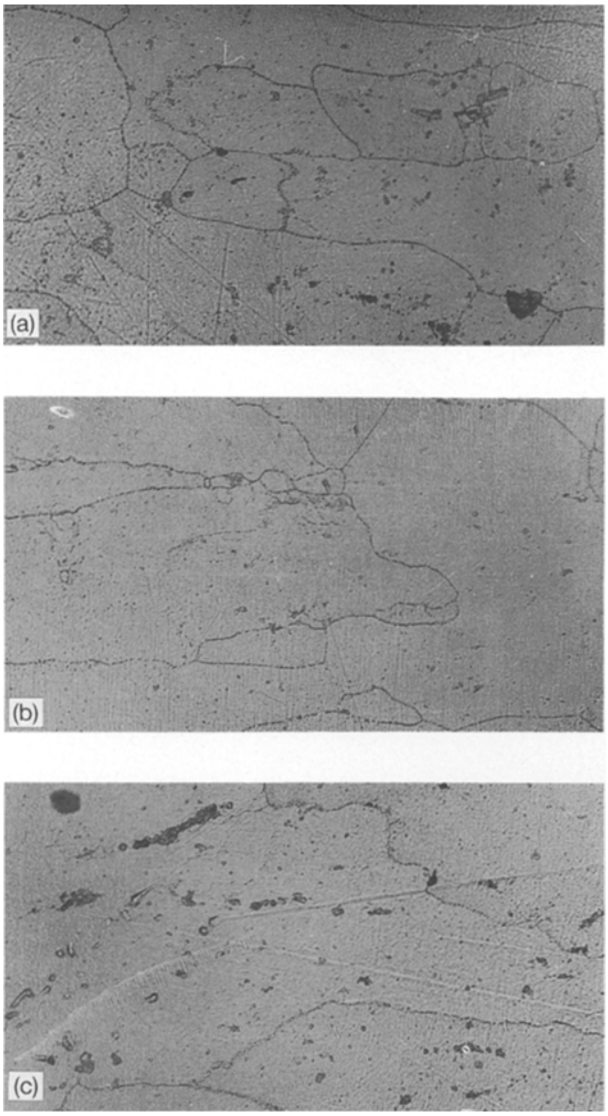

Figure 10 OM image showing the effect of Te on grain growth for three alloys (×400): (a) alloy W, (b) alloy X, and (c) alloy Y.

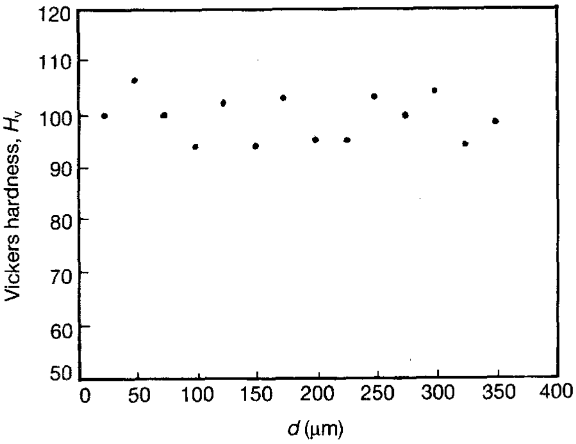

Figure 11 Hardness versus distance from surface of alloy X (solution treated).

a solute depleted surface layer. This depletion of Li atoms from the surface is due to their high diffusivity and affinity to interact with atmospheric oxygen, which leads to hardness deterioration of the surface (Fig. 13). The entrapment of Li atoms by Te atoms also impedes the precipitation process. A further increase of the Te percentage to 0.4 wt % (alloy Y) causes a decrease in tensile strength, hardness and ductility relative to alloy X (0.2% Te) (Figs 4, 7, 14, and 15).

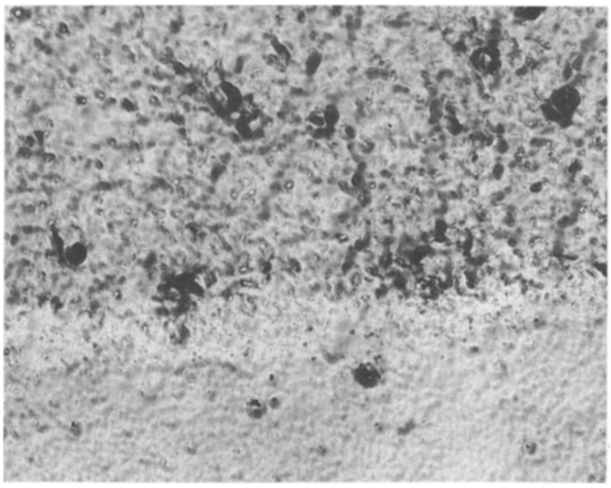

Figure 12 TEM image of depleted surface layer of alloy W (×10 000).

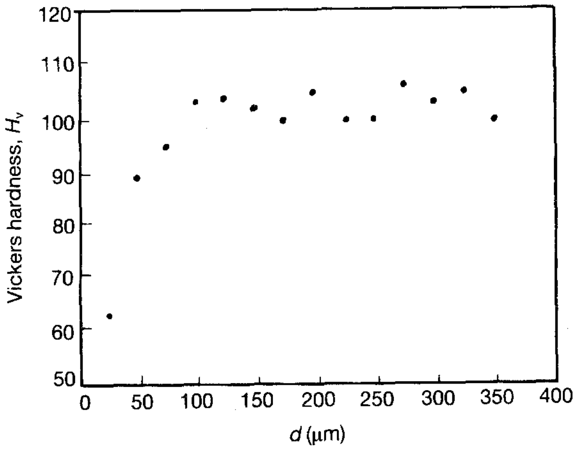

Figure 13 Hardness versus distance from surface of alloy W (solution treated).

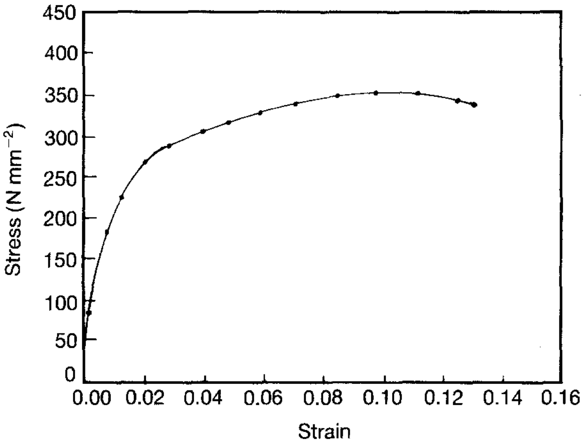

Figure 14 Stress–strain curve of alloy Y.

3.2. Oxidation behaviour

A significant loss of Li from the surface layer during solution treatment of Al–Li based alloys was observed

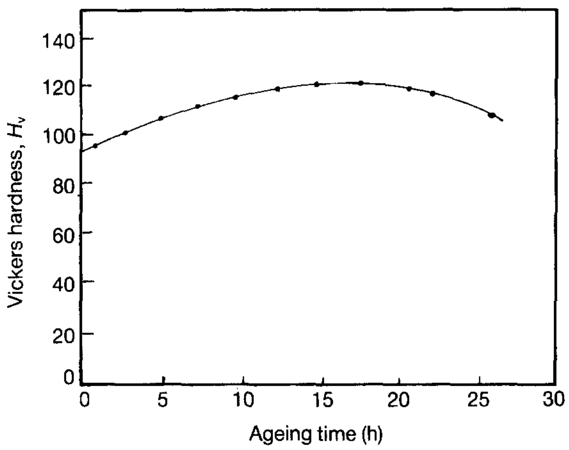

Figure 15 Hardness versus ageing time of alloy Y.

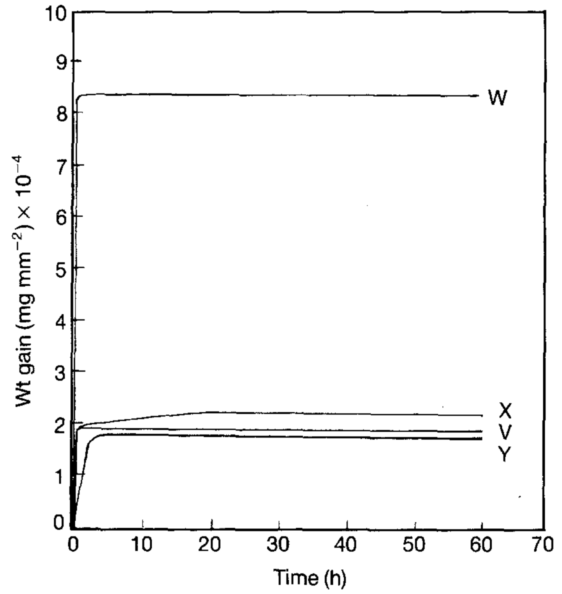

Figure 16 Oxidation behaviour of alloys V, W, X and Y at 300 °C in addition to thermal shocks at 50 and 60 h.

in the present as well as in other works [13, 14, 19]. The extent of the soft layer (≈ 100 μm) in the Te free alloy was consistent with results in [13] and [20]. However, it is not shown in 0.2% Te containing alloy (X), Fig. 11. This could give an indication that Te atoms i.e. up Li atoms and impede them from interaction with atmospheric oxygen as well as other elements in the alloy, resulting in low oxidation and precipitation. It is shown from Figs 16 and 17 that the oxidation of alloy V decreases as the temperature increases. This is due to the increase in alumina (Al_2O_3) content of the scale as oxidation temperature increases, as indicated by X-ray diffractometry. This is because, thermodynamically, the ability of aluminium in reducing the other oxides increases as temperature increases [21, 22]. Aluminium behaves similarly, in some other alloys [23]. In spite of the weight gain of alloy, V is low, but the oxide built on is brittle and of poor adhesion; it cracked and spalled when subjected to thermal stresses, Fig. 18. This is in agreement with other workers, results [11, 24]. However, cracking of the oxide brings the surface of alloy to direct attack of harsh environments which accelerates the attack.

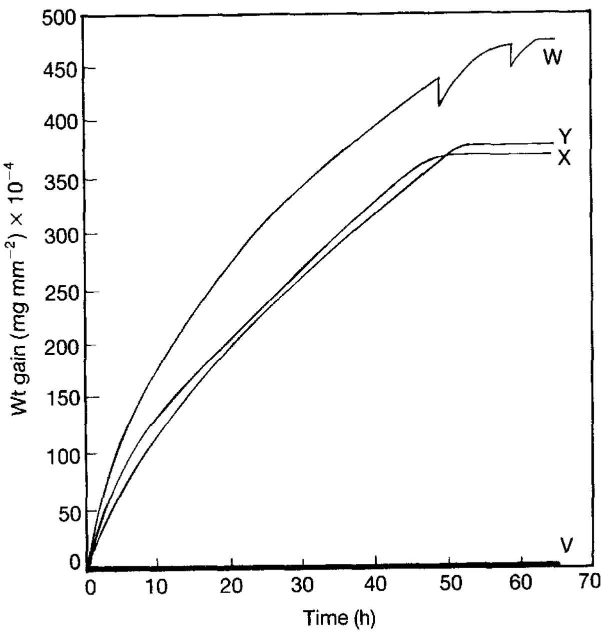

Figure 17 Oxidation behaviour of alloys V, W, X and Y at 500 °C in addition to thermal shocks at 50 and 60 h.

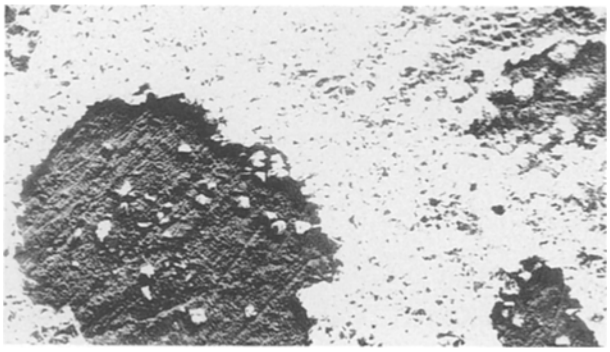

Figure 18 SEM image of cracking and spalling of oxide formed on alloy V due to thermal stresses at 500 °C (× 100).

The results of weight gain for alloy W, the Li containing alloy, are shown in Fig. 16 at 300 °C. The shape of the curve is similar to that of alloy V, the Li free alloy, but the amount of oxidation in W is higher by more than 400% in the present work, which was also predicted by others [12, 14, 15].

At an oxidation temperature of 500 °C, the behaviour of alloy W is different from that of V. The curve for alloy V has zero slope and could not be distinguished from the abscissa, as can be seen in Fig. 17. The introduction of Li (alloy W) results in a different oxidation behaviour, since the weight gain increases with time in a parabolic form. This means that the produced oxide film is porous and unprotective. In addition, the oxide layer does not withstand against thermal shocks at 50 and 60 h. The sharp weight loss that appears means cracking and spalling have taken place, Figs 17 and 19. The spalling was not detected at 300 °C oxidation test. This could be explained by the fact that the oxide layer is too thin and hence more adhesive and protective compared to that produced at 500 °C, as is indicated by the smaller amount of weight gain in addition to its stability within less than 1 h.

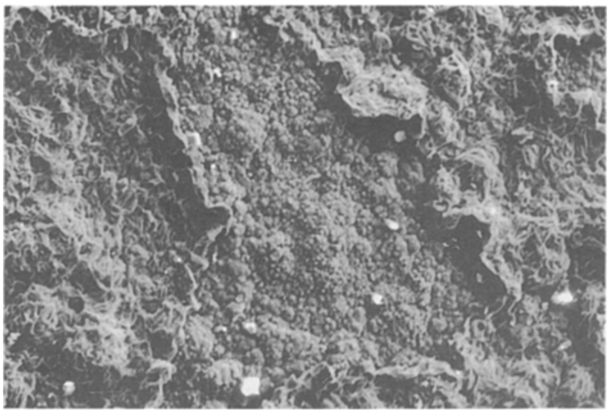

Figure 19 SEM image of cracking and spalling of oxide formed on alloy W due to thermal stresses at 500 °C (× 200).

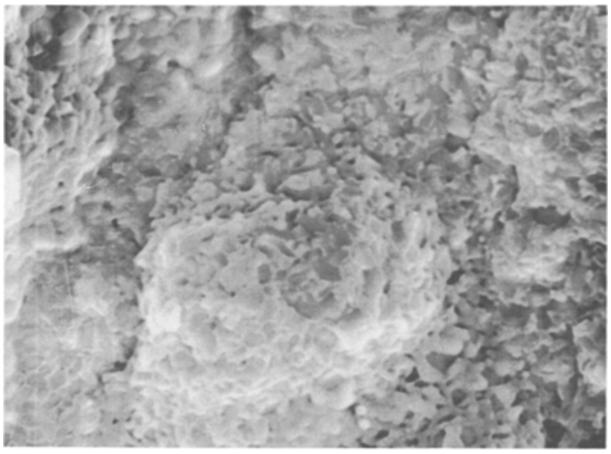

Figure 20 SEM image showing no cracking or spalling due to thermal shocks on oxides formed on alloy X at 500 °C (× 500).

X-ray diffraction studies show that the oxides produced at 300 °C are Li_2Co_3, α-Li_5AlO_4 and γ-$LiAlO_2$, in addition to alumina (Al_2O_3). Alumina, however, disappears at higher temperature (500 °C) but the other oxides are present. This may explain the change in the behaviour of alloy W at 500 °C and also the differences between alloys V and W at 300 °C and 500 °C. This result agrees with other workers [12, 13, 15] as well.

The addition of 0.2 and 0.4 wt % Te to alloy W, to produce alloys X and Y, respectively, substantially reduced the weight gain at 300 °C, Fig. 16. The weight gain of these two alloys stabilized within 30 min and 4 h, respectively. The weight gain in alloy Y, with 0.4 wt % Te, is even lower than that of lithium free aluminium alloy, V. This means that the role of Te in the prevention of oxidation in Al–Li based alloys is very vital, since Li as well as Mg increase the oxidation in Al based alloys [12, 14, 15]. The weight gain was lower than in case of alloy W (Te free alloy) by more than 300% in alloys Y and X.

In a previous study, Field *et al.* [15] reported that under dry air in the 500 and 525 °C temperature range, γ-$LiAlO_2$ is the predominant oxide phase on the Al–2.7 wt % Li. The present results, however, indicate that the dominating reaction product is Li_2CO_3. This is in agreement with Ahmad [13] working on the commercial Al–2.5% Li–1.4% Cu–0.65% Mg–0.14% Zr alloy oxidized in air at 530 °C and at atmospheric pressure.

The oxidation process is accelerated very much at high temperature (500 °C) in alloys W, X and Y. But still the weight gain in alloys X and Y is smaller than that in the corresponding alloy V by about 30% and 30 h oxidation. The effectiveness of 0.4 and 0.2% Te is more or less similar at 500 °C, Fig. 17. The other noticed phenomenon of Te is the stability of weight gain at 500 °C after approximately 52 h for both alloys X and Y. This means that the oxides become nonporous and protective. Quantitative analysis of X-ray diffraction, at 500 °C, shows that Li and Te present in the scales of X and Y alloys and the type of oxides in both alloys are the same.

It was previously found [11] that Ge has some role in inhibiting oxidation in Al–Li based alloys up to 400 °C. On the contrary, the addition of 0.2 wt % Ge accelerates oxidation at 500 °C by about 12% after oxidation for 30 h, beside its limitation is reducing the oxidation at less than 500 °C compared to 0.2 wt % Te addition.

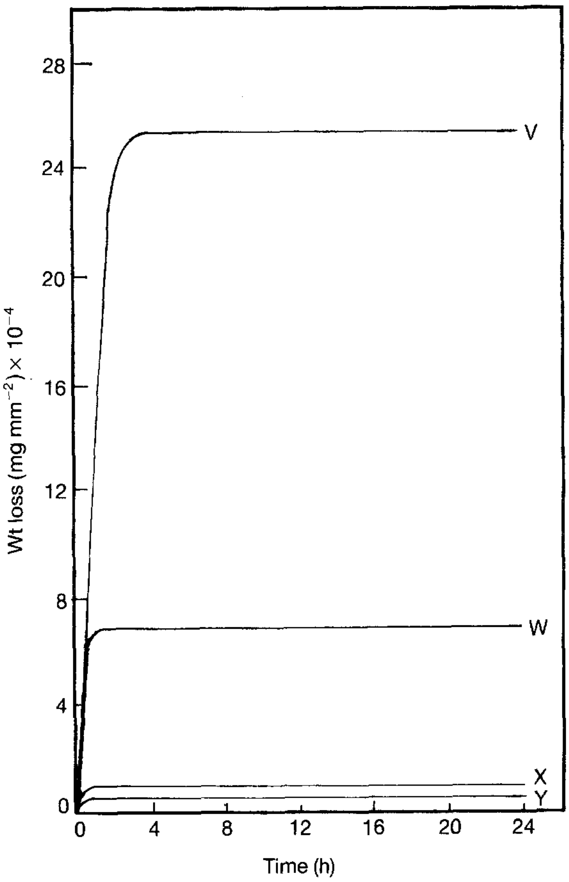

Figure 21 Effects of alloying elements on weight loss due to corrosion–erosion at room temperature.

The oxide layer on alloys X and Y remains sound and unaffected by thermal shock, Fig. 20. It can be therefore concluded that the enhancement of oxide plasticity and adhesion is attributed to the Te effect. This improvement can be explained by the decrease of vacancies at the oxide–metal interface and by modifications of the diffusivity and solubility of alloying elements.

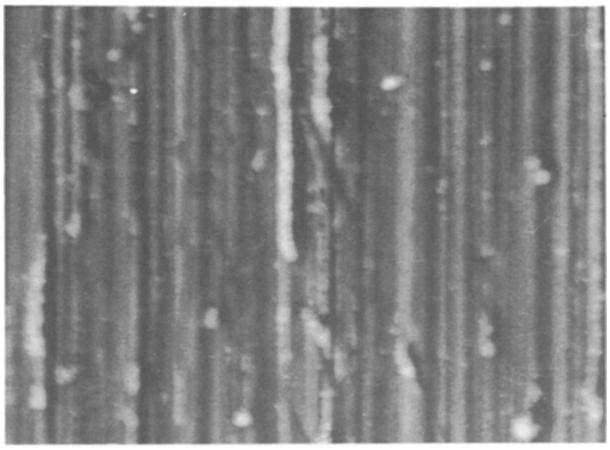

Figure 22 SEM image showing effect of exposure to water jet on alloy X after 25 h at room temperature (× 1500).

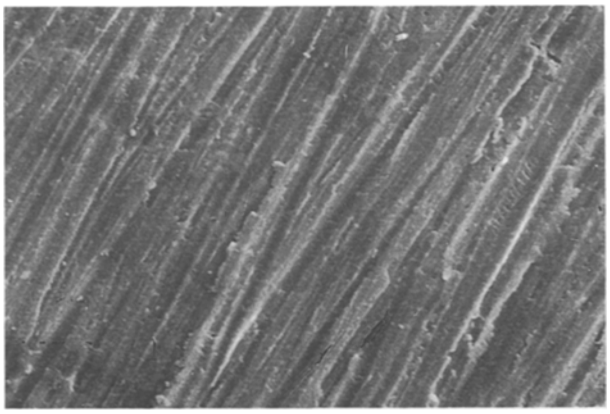

Figure 23 SEM image showing effect of exposure to water jet on alloy Y after 25 h at room temperature (× 1500).

3.3 Corrosion–erosion

The weight losses per unit area per unit time were plotted, in time test, against the exposure time. They were generally similar to the behaviour of some other alloys [25, 26]. A significant improvement is also observed in the corrosion–erosion resistance of alloys X and Y (Figs 21–25). The resistance to corrosion–erosion for alloy X increased by 600 and 2300% relative to alloys W (Te free alloy) and V (Li free alloy) respectively. Whereas the increase in corrosion–erosion resistance for alloy Y over that of alloys W and V was 900 and 3390%, respectively.

In addition to the rate of weight loss reached steady state faster in X and Y, Te containing, alloys than the other alloys, V and W. The improvement in corrosion–erosion resistance means improvement in plasticity and adhesion of oxide scale.

4. Conclusions

1. A great improvement in oxidation resistance took place in X and Y alloys due to trace additions of Te, which were more than 300 and 30% at 300 and 500 °C, respectively.

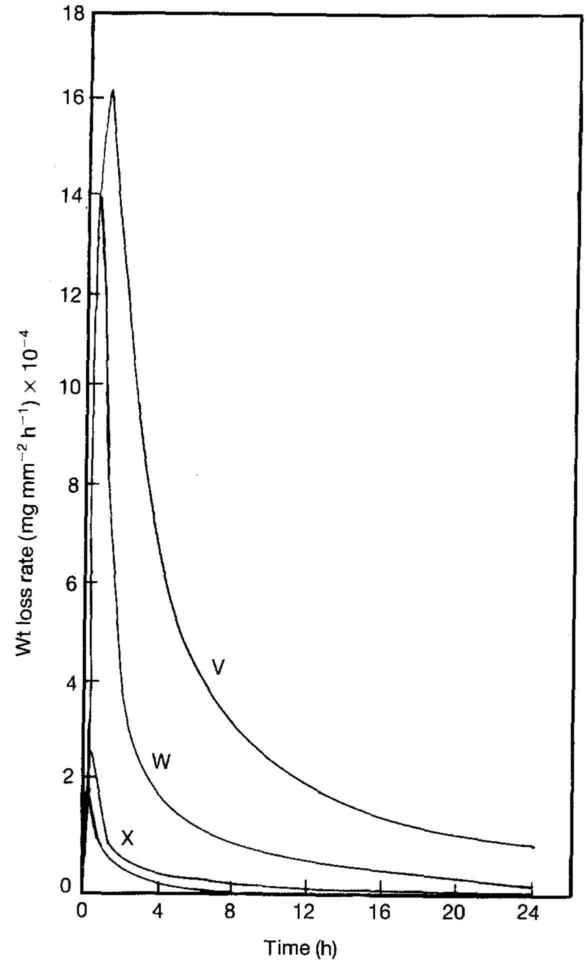

Figure 24 Effects of alloying elements on weight loss rate at room temperature.

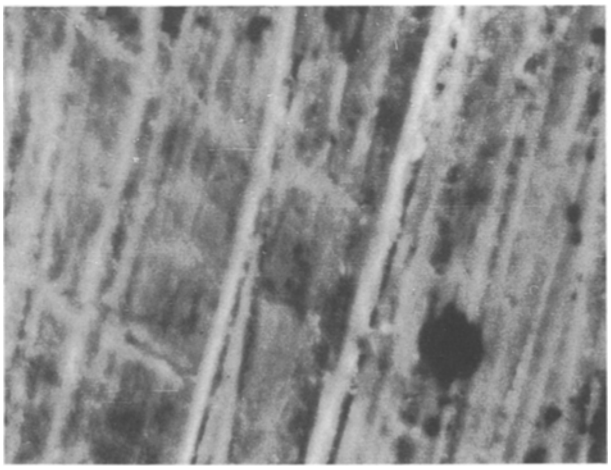

Figure 25 SEM image showing effect of exposure to water jet on alloy W after 25 h at room temperature (× 1500).

2. The addition of 0.4 % Te (alloy Y) decreased oxidation at 300 °C even lower than Li free alloy, V; but its effect was not far away from 0.2 % Te addition, particularly at higher temperature (500 °C) and for longer time.

3. Te additions (alloy X and Y) greatly increased the resistance of oxide (100%) to cracking and spalling during thermal shock.

4. The oxidation rate of alloy V (Li free alloy) decreased as temperature increased. Whereas the oxidation rate of alloys W, X and Y increased as temperature increased.

5. Erosion–corrosion resistance of alloys X and Y were much higher than those of alloys V and W; this means that plasticity and adhesion of the oxide are improved.

6. During solution heat treatment of alloy W a soft surface layer was developed due to the selective oxidation of lithium. This layer does not appear in Te containing alloys.

7. X-ray diffraction analysis of the oxides formed on alloy W revealed the presence of Al_2O_3, Li_2CO_3, α-Li_5AlO_4 and γ-$LiAlO_2$ at 300 °C, whereas alumina disappeared at 500 °C.

8. None of the oxides were detected by X-ray diffractometry in Te containing alloys (X and Y) at 300 °C, whereas at 500 °C all the above oxides were detected.

9. The predominant oxide in W, X and Y at 500 °C was Li_2CO_3.

10. The addition of 0.2 wt % Te (alloy X) increased the ductility by 25% over the corresponding alloy W (Te free alloy) and decreased the strength by less than 8%, i.e. increased the toughness.

11. Thermal stability of alloy X (0.2 % Te) was better than in the case of alloys V, W or even Y (0.4% Te).

References

1. M. H. TOSTEN, S. K. VOSUDEVAN and P. K. HOWELL *Metal. Trans.* **19A** (1988) 51.
2. W. A. CASSADA, G. J. SHIFLET and E. A. STARKE Jr, *Acta Metall.* **34** (1986) 307.
3. J. T. AL-HAIDARY, A. W. BAKRI and A. S. JABUR *Engng Technol* **12** (1993) 89.
4. J. W. MARTIN, *Ann. rev. Mater. Sci.* **18** (1988) 101.
5. K. K. SANKARAN and J. E. O'NEIL in "Second International Al–Li Conference", edited by T. H. Scanders and E. A. Starke (Metallurgical Society AIME, New York, 1984) p. 393.
6. K. F. ASHTON, D. S. THOMPSON, E. A. STARKE and F. S. LIN in "Third International Al-Li Conference", edited by C. E. Baker, P. J. Gregson, S. J. Harris and C. J. Peel (The Institute of Metals, London, 1986) p. 66.
7. C. J. PEEL, B. EVANS, C. A. BAKER, D. A. BENNETT, P. J. GREGSON and H. M. FLOWE in "Second International Al–Li Conference", edited by T. H. Scanders and E. A.. Starke (Metallurgical Society AIME, New York, 1984) p. 363.
8. M. GONCALVES and G. M. SELLARS in "Fourth International Al–Li Conference", Vol. 48, edited by G. Champier, B. Dubost, D. Miannay and L. Sabetay (Journal Physique, Paris, 1987) pp. C3–171.
9. W. S. MILLER, M. P. THOMAS and S. J. LLOYD in "Third International Al–Li Conference", edited by C. E. Baker, P. J. Gregson, S. J. Harris and C. J. Peel (The Institute of Metals, London, 1986) p. 584.
10. A. K. VASUDEVAN and S. SURESH, *Mater. Sci. Engng* **72** (1985) 37.
11. A. BAKRI, J. T. Al-HAIDARY and R. N. RAZODI, *Engng. Technol. J* **11** (1992) 72.
12. M. BURKE and J. M. PAPAZIAN, in "Third International Al–Li Conference", edited by C. E. Baker, P. J. Gregson, S. J. Harris and C. J. Peel (The Institute of Metals, London, 1986) p. 287.
13. M. AHMAD *Metal. Trans.* **18A** (1987) 681.
14. D. J. FIELD, E. P. BUTLER and M. SCAMANS in "First International Al–Li Conference", edited by T. H. Scanders and E. A. Starke (Metallurgical Society AIME, New York, 1981) p. 325.
15. D. J. FIELD, G. M. SCAMANS and E. P. BUTLER in "Second International Al–Li Conference", edited by T. H. Scanders and B. A. Starke (Metallurgical Society AIME, New York, 1984) p. 657.
16. D. B. WILLIAMS and J. W. EDINGTON, *Metal. Sci.* **9** (1975) 529.
17. ASM, "Aluminum" edited by K. R. Van Horn, Vol. 1, (American Society for Metals, Metals Park, OH, 1967) p. 207.
18. H. J. AXON and W. HUME-ROTHERY, *Proc. R. Soc., Lond.* **193A** (1948) 1.
19. J. M. PAPAZIAN, R. L. SCHULTE and P. N. ADLER, *Metal. Trans.* **17A** (1986) 635.
20. B. JAENSSON Report TKFB-84. 094, (Saab-Scania A. B., 1984) p. 1.
21. N. BRIKS and G. H. MEIER, "Introduction to High Temperature Oxidation of Metals", 1st Edn, (Edward Arnold, 1974) p. 31.
22. J. C. SCULLY, "The Fundamentals of Corrosion", 2nd Edn, (Pergamon International, 1975).
23. G. C. WOOD, *Oxid. Metal.* **2** (1970) 11.
24. H. E. EVANS and C. LOBB, *Corr. Sci.* **24** (1984) 209.
25. W. H. ALLOR "Atmospheric Corrosion" (Wiley Interscience, 1982) p. 297.
26. E. RABINOWICZ "Friction and Wear of Materials" (Wiley, 1965) p. 186.

Received 13 July 1993
and accepted 28 June 1994